

**Table 2** FRET between PS1 N-terminus and APP CT in NcadCHOSw cells treated with N-cadherin neutralizing GC-4 antibody or IgG as a control

Cell line	FRET donor (Alexa 488)	FRET acceptor (Cy3)	Alexa 488 lifetime in ps (mean ± SE)	<i>p</i> value (compared with control IgG)
NcadCHOSw (Negative Control)	PS1 NT	None	1903 ± 28	<i>p</i> < 0.01
NcadCHOSw with control IgG ( <i>n</i> = 21)	PS1 NT	APP CT	1677 ± 22	
NcadCHOSw with GC-4 ( <i>n</i> = 17)	PS1 NT	APP CT	1789 ± 100	

**Table 3** FRET between PS1 loop and APP CT in living NcadCHOSw cells treated with GC-4 or IgG

Cell line	FRET donor	FRET acceptor	Alexa 488 lifetime in ps (mean ± SE)	<i>p</i> value (compared with control IgG)
NcadCHOSw (Negative Control)	APP-GFP	None	2076 ± 62	<i>p</i> < 0.01
NcadCHOSw with control IgG ( <i>n</i> = 21)	APP-GFP	PS1-RFP(loop)	1646 ± 223	
NcadCHOSw with GC-4 ( <i>n</i> = 17)	APP-GFP	PS1-RFP(loop)	1859 ± 74	

with tighter cell-cell adhesion mediated by N-cadherin is due to a conformational change in PS1/ $\gamma$ -secretase. The proximity between PS1 NT and CT in fixed and detergent permeabilized cells was evaluated by measuring lifetime of the Alexa 488 donor fluorophore (PS1 NT Alexa 488) in the absence (negative control) and presence of the Cy3 acceptor on the PS1 CT. As expected, the Alexa 488 donor fluorophore lifetime shortened when the PS1 CT was labeled with the Cy3 acceptor (Table 4), consistent with the close proximity between the PS1 NT and CT in APPSw-CHO cells. In contrast, Alexa 488 lifetime in APPSw/Ncad-CHO cells was significantly longer (1821 ± 14 ps), compared with that in APPSw-CHO cells, indicating that N-cadherin 'opened' the PS1 conformation with NT and CT being further apart (Tables 2 and 3, Fig. 3c and d). Thus, these results are in agreement with the previous findings that more 'open' PS1 conformation correlates with generation of the shorter A $\beta$  species (Leo *et al.* 2004), and therefore decreased A $\beta_{42/40}$  ratio in APPSw/Ncad-CHO cells may be attributed to the change in conformation of the PS1/ $\gamma$ -secretase due to N-cadherin over-expression.

#### PS1/N-cadherin interaction affects both A $\beta$ production and A $\beta_{42/40}$ ratio

Since N-cadherin interacts with the cytoplasmic loop of PS1 CTF (Georgakopoulos *et al.* 1999), we next deter-

mined whether the PS1/N-cadherin interaction affects A $\beta$  production and/or A $\beta_{42/40}$  ratio. To test this, either wtPS1 or a PS1 mutant lacking the N-cadherin interaction domain [ $\Delta$ 340-350PS1, Uemura *et al.* 2007] was transfected into APPSw/Ncad-CHO cells. Since PS1/ $\gamma$ -secretase acts in a complex including PS1, Nicastrin, Pen-2 and Aph-1 (Takasugi *et al.* 2003),  $\Delta$ 340-350PS1 competes with endogenous wild-type PS1 to occupy other components of  $\gamma$ -secretase and act in a dominant-negative fashion (Thinakaran *et al.* 1997). As expected, immunoprecipitation assay revealed that  $\Delta$ 340-350PS1 does not interact with N-cadherin (Fig. 4a). We found that the extracellular levels of both A $\beta_{40}$  (Fig. 4b) and A $\beta_{42}$  (Fig. 4c) were decreased after the transient expression of  $\Delta$ 340-350PS1, compared with wtPS1. In addition, A $\beta_{42/40}$  ratio in the medium was increased in the  $\Delta$ 340-350PS1 transfectants, compared with that in wtPS1 (Fig. 4d), indicating that the PS1/N-cadherin interaction affects both A $\beta$  production and A $\beta_{42/40}$  ratio.

#### Discussion

In this report, we demonstrate that introducing N-cadherin into cadherin-deficient CHO cells increased secreted A $\beta_{40}$  and A $\beta_{42}$  levels (Fig. 2). The expression of N-cadherin in CHO cells elevates cell-surface levels of PS1/ $\gamma$ -secretase [Uemura *et al.* 2007], see also Fig. 1. Thus, the effect of

**Table 4** FRET between PS1 NT and CT in CHOSw compared with NcadCHOSw cells

Cell line	FRET donor (Alexa 488)	FRET acceptor (Cy3)	Alexa 488 lifetime in ps (mean ± SE)	<i>p</i> value (compared with NcadCHOSw)
APPSw-CHO ( <i>n</i> = 11)	PS1 NT	None (negative control)	1897 ± 7	<i>p</i> < 0.0001
APPSw-CHO ( <i>n</i> = 14)	PS1 NT	PS1 CT	1524 ± 46	<i>p</i> = 0.0002
APPSw/Ncad-CHO ( <i>n</i> = 14)	PS1 NT	PS1 CT	1821 ± 14	

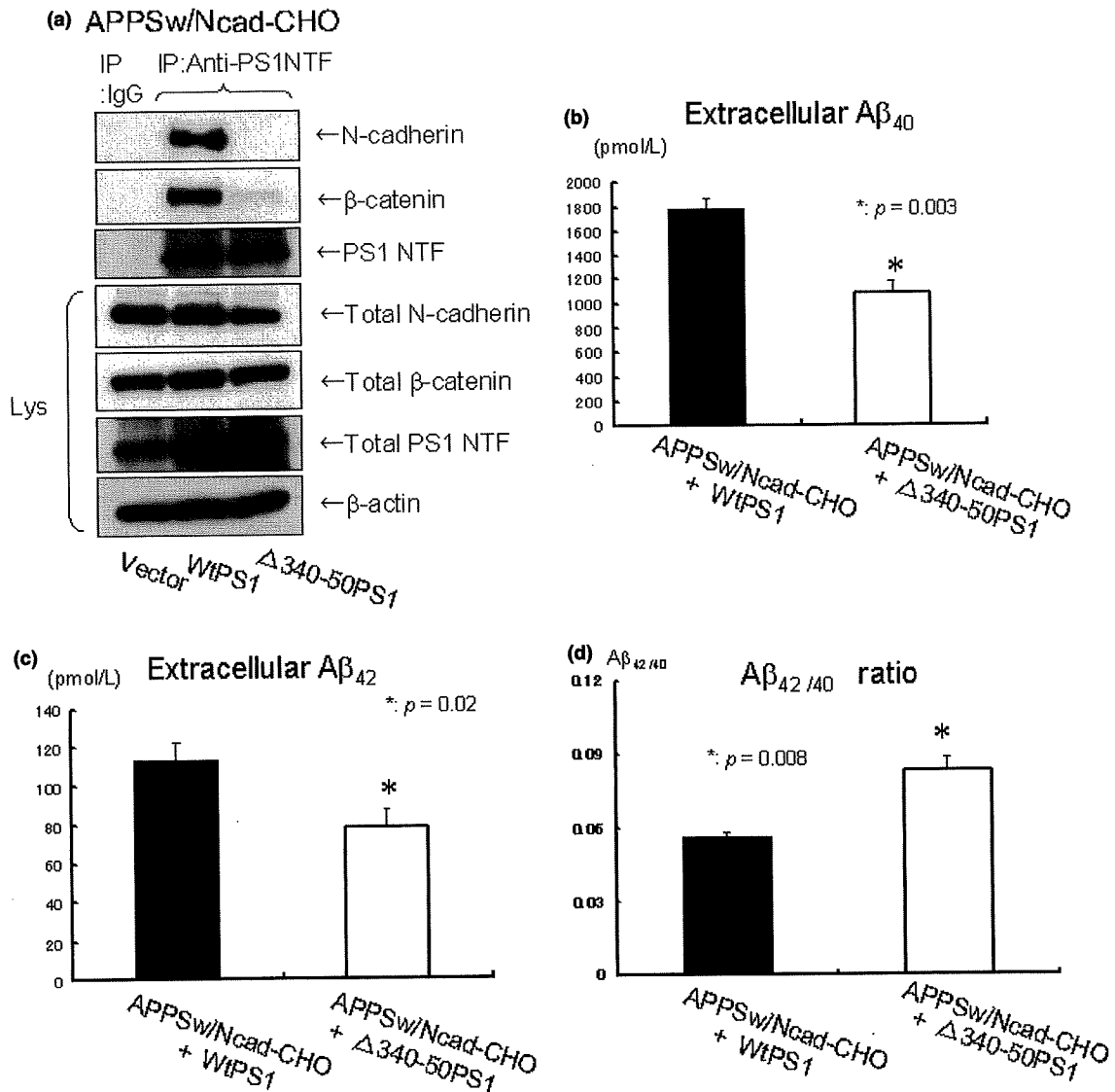


**Fig. 4** Loss of PS1/N-cadherin interaction reduces extracellular A $\beta$  levels and enhances A $\beta_{42/40}$  ratio. (a) APPSw/Ncad-CHO cells were transfected with either wtPS1 or PS1 mutant lacking PS1/N-cadherin interaction domain ( $\Delta$ 340-350PS1). 24 h after transfection, cell lysates were immunoprecipitated with rabbit polyclonal anti-PS1 NT antibody or normal rabbit IgG as a control, followed by the western blot. N-cadherin and  $\beta$ -catenin were efficiently co-immunoprecipitated with wild type PS1. However, very poor N-cadherin and  $\beta$ -catenin signal was detected in the co-immunoprecipitates from APPSw/Ncad-CHO cells transfected with  $\Delta$ 340-350PS1, indicating the lack of PS1/N-cadherin/ $\beta$ -catenin interaction. The expression levels of PS1, N-cadherin and  $\beta$ -catenin in the cell lysates (Lys) were similar between these cell lines. The bottom lane indicates the  $\beta$ -actin level, used as a loading control. (b)  $6 \times 10^5$  of APPSw/Ncad-CHO cells cultured in

the cadherin expression on A $\beta$  secretion might be mediated by the change in the subcellular distribution of PS1/ $\gamma$ -secretase. In addition, our FLIM analysis revealed

that the N-cadherin expression allowed more PS1 and APP to interact near the cell surface, resulting in a greater amount of fluorophore-labeled epitopes coming into close

3.5 cm dish were transfected with either wtPS1 or PS1 mutant lacking PS1/N-cadherin interaction domain ( $\Delta$ 340-350PS1). 24 h after transfection, cells were washed once with OPTI-MEM and incubated in fresh OPTI-MEM for 12 h. After incubation, the culture medium was collected and the amount of extracellular A $\beta_{40}$  was measured by ELISA. Extracellular A $\beta_{40}$  was significantly reduced in the background of  $\Delta$ 340-350PS1 transfection, compared with that in wtPS1 transfected cells (\* $p = 0.003$ ,  $n = 4$ ). (c) The amount of extracellular A $\beta_{42}$  in the same condition as in (b) was measured by ELISA. Extracellular A $\beta_{42}$  was significantly reduced in the background of  $\Delta$ 340-350PS1 transfection, compared with that in wtPS1 transfected cells (\* $p = 0.02$ ,  $n = 4$ ). (d) The A $\beta_{42/40}$  ratio in the conditions (b) and (c) was significantly reduced in the background of  $\Delta$ 340-350PS1 transfection (\* $p = 0.008$ ,  $n = 4$ ).

proximity (Table 1 and see more red pixels in Fig. 3b compared with 3a). The FLIM results were confirmed by co-IP experiment (Supporting information Fig. S2), indicating better accessibility of APP to PS1/ $\gamma$ -secretase in the presence of N-cadherin. These data suggest that subcellular redistribution and better accessibility of PS1/ $\gamma$ -secretase to APP substrate may be the cause of the net increase in total A $\beta$  production in the presence of N-cadherin. The cellular compartment in which APP/PS1 interactions are promoted by N-cadherin was not clarified in the present study. However, since N-cadherin is an important cell adhesion molecule and we have previously demonstrated that N-cadherin promotes cell-surface expression of PS1/ $\gamma$ -secretase ((Uemura *et al.* 2007), see also Fig. 1), the interactions are likely to occur near to the cell surface.

Interestingly, N-cadherin expression not only enhanced A $\beta$  release, but also decreased A $\beta_{42/40}$  ratio, the latter effect is similar to NSAIDs treatment (Leo *et al.* 2004) and opposite to that caused by the FAD-linked PS1 mutations (Berezovska *et al.* 2005). This effect was associated with the 'open' PS1 conformation, driving NT and CT further apart, in N-cadherin expressing cells as revealed by the FLIM assay (Tables 2 and 3 and Fig. 3c and d). Preventing N-cadherin-PS1 interaction either by absence of N-cadherin (Fig. 1) or by introducing a PS1 mutant that does not interact with N-cadherin (Fig. 4) both have increased A $\beta_{42/40}$  ratio. In the absence of N-cadherin (APPSw-CHO cells), the A $\beta_{42/40}$  ratio was around  $0.095 \pm 0.006$ , whereas it was reduced to  $0.072 \pm 0.006$  in the presence of N-cadherin (APPSw/Ncad-CHO cells) (Fig. 2c). The A $\beta_{42/40}$  ratio under the expression of  $\Delta 340$ -350PS1 was  $0.083 \pm 0.009$ , whereas A $\beta_{42/40}$  ratio under the expression of wt PS1 was  $0.056 \pm 0.004$  (Fig. 4d). These results indicate that  $\Delta 340$ -350 mutant prevented the decrease in A $\beta_{42/40}$  ratio induced by N-cadherin expression and restored to baseline A $\beta_{42/40}$  ratio. Since N-cadherin binds to the cytoplasmic loop of PS1 CT (Georgakopoulos *et al.* 1999), it is possible that this physical contact causes an allosterical change in PS1 conformation by moving PS1 NT and CT further apart. On the contrary to the N-cadherin expression, the expression of wt PS1 has no effect on A $\beta$  production. Other reports have also demonstrated that single expression of wt PS1 has limited effect on A $\beta$  production *in vivo* (Citron *et al.* 1997). We speculate that this apparent contradiction is caused by the lack of other  $\gamma$ -secretase components, when PS1 is expressed alone.  $\gamma$ -secretase is composed of PS1, nicastrin, pen-2 and aph-1 and can remain stable only when these components are available. It was also reported that expression of pen-2 is required for conferring the  $\gamma$ -secretase activity and endoproteolysis of PS1 (Takasugi *et al.* 2003). Thus, expression of PS1 alone might not have impact on A $\beta$  metabolism significantly.

Thus, expression of N-cadherin modulates A $\beta$  production in two ways: the total amount of A $\beta$  and the A $\beta_{42/40}$  ratio. These are independent readouts of  $\gamma$ -secretase function. According to our experimental data, these changes can be interpreted as reflecting access of N-terminally cleaved APP to functionally active  $\gamma$ -secretase (total amount of A $\beta$ ) compared with the exact molecular interaction between PS-1 and the APP substrate (A $\beta_{42/40}$  ratio). The presence of N-cadherin impacts each of these features, by directing the localization of  $\gamma$ -secretase closer to cell surface membrane as well as a direct allosteric effect on PS-1/ $\gamma$ -secretase conformation. Accumulating evidence suggests that partial loss of function in PS1/ $\gamma$ -secretase may lead to increased A $\beta_{42/40}$  ratio as well as to neurodegeneration (Shen and Kelleher 2007; Wolfe 2007). In addition, a recent report suggests that A $\beta_{40}$  may inhibit amyloid deposition and thus may be physiologically neuroprotective (Kim *et al.* 2007). In this respect, tight cell-cell contact may enhance the function of PS1/ $\gamma$ -secretase to produce more A $\beta_{40}$  by inducing its distributional and conformational change.

It has recently been shown that neuronal activity modulates the production and secretion of A $\beta$  peptides (Kamenetz *et al.* 2003; Lesne *et al.* 2005). In addition, it was demonstrated *in vivo* that A $\beta$  levels in the brain interstitial fluid are dynamically influenced by synaptic activity (Cirrito *et al.* 2005). Taken together, A $\beta$  secretion seems to be physiologically regulated in neurons and A $\beta$  itself may have its own physiological function (Pearson and Peers 2006). On the contrary, converging lines of evidence suggests that natural soluble A $\beta$  oligomers trigger synaptic loss (Spires *et al.* 2005; Shankar *et al.* 2007). Therefore, it is plausible that synaptic dissociation caused by A $\beta$  oligomers changes PS1 conformation to produce more A $\beta_{42}$ , thus starting the vicious cycle of A $\beta_{42}$  generation by modifying the A $\beta_{42/40}$  ratio. Our present study presents solid evidence that A $\beta$  production and the A $\beta_{42/40}$  ratio can be modulated by the degree of PS1-N-cadherin interaction, and thus potentially by cell-cell adhesion status. Our current findings, thus, provide a potential link between synaptic contacts and physiological A $\beta$  release, with cadherins being the key player. However, these experiments are carried out by CHO cell lines exogenously expressed with APP or its mutant, which does not allow to conclude about the relevance of the presented mechanism in neurons and remain to be proved in neuron and *in vivo* settings.

With its potential role in the rearrangement of existing cell-cell contacts (Okamoto *et al.* 2001; Marambaud *et al.* 2002; Haas *et al.* 2005) PS1/ $\gamma$ -secretase may influence synaptic plasticity, which might be affected in AD. Future study in this field could lead to a better understanding of AD synaptic pathophysiology.

## Acknowledgments

Research described in this article was supported by Philip Morris USA Inc., Philip Morris International (OB, SS) and NIH AG026593 (OB) and by the Ministry of Education, Science, Sports and Culture (Japan), Grant-in-Aid for 18023021, 18059019 (AK). We thank Dr Kaether (Ludwig-Maximilians University, Germany) for generously providing original PS1-GFP construct.

## Supporting information

Additional Supporting information may be found in the online version of this article:

**Fig. S1** N-cadherin expression reduces A $\beta$ <sub>42/40</sub> ratio in the background of wild-type APP expression.

**Fig. S2** N-cadherin expression increases APP-PS1 interaction.

Please note: Wiley-Blackwell are not responsible for the content or functionality of any supplementary materials supplied by the authors. Any queries (other than missing material) should be directed to the corresponding author for the article.

## References

- Berezovska O., Ramdya P., Skoch J., Wolfe M. S., Bacskai B. J. and Hyman B. T. (2003) Amyloid precursor protein associates with a nicastrin-dependent docking site on the presenilin 1-gamma-secretase complex in cells demonstrated by fluorescence lifetime imaging. *J. Neurosci.* **23**, 4560–4566.
- Berezovska O., Lleo A., Herl L. D., Frosch M. P., Stern E. A., Bacskai B. J. and Hyman B. T. (2005) Familial Alzheimer's disease presenilin 1 mutations cause alterations in the conformation of presenilin and interactions with amyloid precursor protein. *J. Neurosci.* **25**, 3009–3017.
- Bozdagi O., Shan W., Tanaka H., Benson D. L. and Huntley G. W. (2000) Increasing numbers of synaptic puncta during late-phase LTP: N-cadherin is synthesized, recruited to synaptic sites, and required for potentiation. *Neuron* **28**, 245–259.
- Cirrito J. R., Yamada K. A., Finn M. B., Sloviter R. S., Bales K. R., May P. C., Schoepp D. D., Paul S. M., Mennerick S. and Holtzman D. M. (2005) Synaptic activity regulates interstitial fluid amyloid-beta levels in vivo. *Neuron* **48**, 913–922.
- Citron M., Westaway D., Xia W. *et al.* (1997) Mutant presenilins of Alzheimer's disease increase production of 42-residue amyloid beta-protein in both transfected cells and transgenic mice. *Nat. Med.* **3**, 67–72.
- De Strooper B., Saftig P., Craessaerts K., Vanderstichele H., Guhde G., Annaert W., Von Figura K. and Van Leuven F. (1998) Deficiency of presenilin-1 inhibits the normal cleavage of amyloid precursor protein. *Nature* **391**, 387–390.
- De Wever O., Westbroek W., Verloes A., Bloemen N., Bracke M., Gespach C., Bruyneel E. and Mareel M. (2004) Critical role of N-cadherin in myofibroblast invasion and migration in vitro stimulated by colon-cancer-cell-derived TGF-beta or wounding. *J. Cell Sci.* **117**, 4691–4703.
- Georgakopoulos A., Marambaud P., Efthimiopoulos S. *et al.* (1999) Presenilin-1 forms complexes with the cadherin/catenin cell-cell adhesion system and is recruited to intercellular and synaptic contacts. *Mol. Cell* **4**, 893–902.
- Haas I. G., Frank M., Veron N. and Kemler R. (2005) Presenilin-dependent processing and nuclear function of gamma-protocadherins. *J. Biol. Chem.* **280**, 9313–9319.
- Isoo N., Sato C., Miyashita H., Shinohara M., Takasugi N., Morohashi Y., Tsuji S., Tomita T. and Iwatsubo T. (2007) Abeta42 overproduction associated with structural changes in the catalytic pore of gamma-secretase: common effects of Pen-2 N-terminal elongation and fenofibrate. *J. Biol. Chem.* **282**, 12388–12396.
- Kamenetz F., Tomita T., Hsieh H., Seabrook G., Borchelt D., Iwatsubo T., Sisodia S. and Malinow R. (2003) APP processing and synaptic function. *Neuron* **37**, 925–937.
- Kim J., Onstead L., Randle S., Price R., Smithson L., Zwizinski C., Dickson D. W., Golde T. and McGowan E. (2007) Abeta40 inhibits amyloid deposition in vivo. *J. Neurosci.* **27**, 627–633.
- Kinoshita A., Whelan C. M., Smith C. J., Berezovska O. and Hyman B. T. (2002) Direct visualization of the gamma secretase-generated carboxyl-terminal domain of the amyloid precursor protein: association with Fe65 and translocation to the nucleus. *J. Neurochem.* **82**, 839–847.
- Lesne S., Ali C., Gabriel C., Croci N., MacKenzie E. T., Glabe C. G., Plotkine M., Marchand-Verrecchia C., Vivien D. and Buisson A. (2005) NMDA receptor activation inhibits alpha-secretase and promotes neuronal amyloid-beta production. *J. Neurosci.* **25**, 9367–9377.
- Lleo A., Berezovska O., Herl L., Raju S., Deng A., Bacskai B. J., Frosch M. P., Irizarry M. and Hyman B. T. (2004) Nonsteroidal anti-inflammatory drugs lower Abeta42 and change presenilin 1 conformation. *Nat. Med.* **10**, 1065–1066.
- Marambaud P., Shioi J., Serban G. *et al.* (2002) A presenilin-1/gamma-secretase cleavage releases the E-cadherin intracellular domain and regulates disassembly of adherens junctions. *EMBO J.* **21**, 1948–1956.
- Okamoto I., Kawano Y., Murakami D., Sasayama T., Araki N., Miki T., Wong A. J. and Saya H. (2001) Proteolytic release of CD44 intracellular domain and its role in the CD44 signaling pathway. *J. Cell Biol.* **155**, 755–762.
- Pearson H. A. and Peers C. (2006) Physiological roles for amyloid beta peptides. *J. Physiol.* **575**, 5–10.
- Shankar G. M., Bloodgood B. L., Townsend M., Walsh D. M., Selkoe D. J. and Sabatini B. L. (2007) Natural oligomers of the Alzheimer amyloid-beta protein induce reversible synapse loss by modulating an NMDA-type glutamate receptor-dependent signaling pathway. *J. Neurosci.* **27**, 2866–2875.
- Shen J. and Kelleher R. J. (2007) The presenilin hypothesis of Alzheimer's disease: evidence for a loss-of-function pathogenic mechanism. *Proc. Natl. Acad. Sci. USA* **104**, 403–409.
- Spires T. L., Meyer-Luehmann M., Stern E. A., McLean P. J., Skoch J., Nguyen P. T., Bacskai B. J. and Hyman B. T. (2005) Dendritic spine abnormalities in amyloid precursor protein transgenic mice demonstrated by gene transfer and intravital multiphoton microscopy. *J. Neurosci.* **25**, 7278–7287.
- Takasugi N., Tomita T., Hayashi I., Tsuruoka M., Niimura M., Takahashi Y., Thinakaran G. and Iwatsubo T. (2003) The role of presenilin cofactors in the gamma-secretase complex. *Nature* **422**, 438–441.
- Thinakaran G., Borchelt D. R., Lee M. K. *et al.* (1996) Endoproteolysis of presenilin 1 and accumulation of processed derivatives in vivo. *Neuron* **17**, 181–190.
- Thinakaran G., Harris C. L., Ratovitski T., Davenport F., Slunt H. H., Price D. L., Borchelt D. R. and Sisodia S. S. (1997) Evidence that levels of presenilins (PS1 and PS2) are coordinately regulated by competition for limiting cellular factors. *J. Biol. Chem.* **272**, 28415–28422.
- Togashi H., Abe K., Mizoguchi A., Takaoka K., Chisaka O. and Takeichi M. (2002) Cadherin regulates dendritic spine morphogenesis. *Neuron* **35**, 77–89.
- Uemura K., Kitagawa N., Kohno R., Kuzuya A., Kageyama T., Chonabayashi K., Shibasaki H. and Shimohama S. (2003) Presenilin 1 is involved in maturation and trafficking of N-cadherin to the plasma membrane. *J. Neurosci. Res.* **74**, 184–191.

- Uemura K., Kihara T., Kuzuya A., Okawa K., Nishimoto T., Bito H., Ninomiya H., Sugimoto H., Kinoshita A. and Shimohama S. (2006a) Activity-dependent regulation of beta-catenin via epsilon-cleavage of N-cadherin. *Biochem. Biophys. Res. Commun.* **345**, 951–958.
- Uemura K., Kihara T., Kuzuya A., Okawa K., Nishimoto T., Ninomiya H., Sugimoto H., Kinoshita A. and Shimohama S. (2006b) Characterization of sequential N-cadherin cleavage by ADAM10 and PS1. *Neurosci. Lett.* **402**, 278–283.
- Uemura K., Kuzuya A., Shimozone Y., Aoyagi N., Ando K., Shimohama S. and Kinoshita A. (2007) GSK3beta Activity Modifies the Localization and Function of Presenilin 1. *J. Biol. Chem.* **282**, 15823–15832.
- Wolfe M. S. (2007) When loss is gain: reduced presenilin proteolytic function leads to increased Abeta42/Abeta40. Talking Point on the role of presenilin mutations in Alzheimer disease. *EMBO Rep* **8**, 136–140.



Contents lists available at ScienceDirect

# Autonomic Neuroscience: Basic and Clinical

journal homepage: [www.elsevier.com/locate/autneu](http://www.elsevier.com/locate/autneu)

## Autoimmune autonomic ganglionopathy with Sjögren's syndrome: Significance of ganglionic acetylcholine receptor antibody and therapeutic approach

Takayuki Kondo<sup>a</sup>, Haruhisa Inoue<sup>a,\*</sup>, Takashi Usui<sup>b</sup>, Tsuneyo Mimori<sup>b</sup>, Hidekazu Tomimoto<sup>a</sup>, Steven Vernino<sup>c</sup>, Ryosuke Takahashi<sup>a</sup>

<sup>a</sup> Department of Neurology, Kyoto University Hospital, Kyoto, Japan

<sup>b</sup> Department of Rheumatology and Clinical Immunology, Kyoto University Hospital, Kyoto, Japan

<sup>c</sup> University of Texas Southwestern Medical Center, Dallas, TX, USA

### ARTICLE INFO

#### Article history:

Received 4 August 2008

Received in revised form 29 November 2008

Accepted 1 December 2008

#### Keywords:

Ganglionic acetylcholine receptor antibody

Autoimmune autonomic ganglionopathy

Sjögren's syndrome

Prednisolone

### ABSTRACT

Autoimmune autonomic ganglionopathy (AAG) is a disorder defined by antibodies to the nicotinic acetylcholine receptor of the autonomic ganglia. We report two patients with chronically progressing dysautonomia with Sjögren's syndrome (SS). The first case showed elevated titer of ganglionic acetylcholine receptor (AChR) antibody and improved with oral intake of prednisolone. In contrast, the second case showed no elevation of ganglionic AChR antibody titer and had poor response to immunomodulatory therapy. These two cases indicate that chronic AAG may be treatable by immunomodulatory therapy, and have relevance to SS.

© 2008 Elsevier B.V. All rights reserved.

### 1. Introduction

Peripheral autonomic failures have various backgrounds such as diabetes mellitus, amyloidosis, inherited autonomic neuropathy or autoimmune disorders (e.g. Guillain-Barré syndrome, paraneoplastic syndrome, Sjögren's syndrome etc.). In this decade Vernino et al. proposed a novel disease entity of autoimmune autonomic failure, characterized by positive ganglionic acetylcholine receptor (AChR) antibody in the serum (Vernino et al., 2000) and designated autoimmune autonomic ganglionopathy (AAG). Ganglionic AChR antibody binds to alpha 3 subunits of the nicotinic acetylcholine receptor, which is localized to the postsynaptic neuron in the autonomic nerve ganglion, and disturbs the function of postganglionic autonomic nerves. Serum levels of the ganglionic AChR antibody significantly correlates with both neurological severity and clinical course (high titer; severe symptoms with acute or subacute progression, low titer; mild symptoms with chronic progression) (Low et al., 2003).

Here we present two Japanese patients with Sjögren's syndrome (SS), who also developed gradually progressive autonomic dysfunction. Detailed evaluation revealed clear differences between these two similar cases; one showed elevated titer of ganglionic AChR antibody, improved by oral prednisolone, whereas the other did not show elevation of ganglionic AChR antibody titer and had poor response to

immunomodulatory therapy. In the analysis of these two patients, we discussed the potential relationships between ganglionic AChR and SS.

### 2. Case presentation

#### 2.1. Patient 1

A 74-year-old healthy man has suffered from oral sicca symptom and chronically progressive orthostatic dizziness for 3 years. When changing from the supine to the standing position, he lost consciousness and his blood pressure became too low to be measured. Physiological evaluation revealed orthostatic hypotension (supine position; blood pressure 90/60 mmHg and heart rate 61/min, standing position; 40/30 mmHg and 63/min), tonic pupil (3/3 mm), dry mouth, dry skin, urinary frequency (more than 6 times a night) and constipation. There were no other abnormal findings on neurologic examination. Routine laboratory examinations of blood, CSF and urine showed no abnormal findings. Anti muscarinic acetylcholine receptor M3 antibody was not examined. Plasma noradrenaline concentration decreased to 116 pg/ml (normal 140–570) at rest and failed to respond to tilting. There was no conspicuous abnormality in brain magnetic resonance imaging (MRI), single photon emission computed tomography (IMP-SPECT; imaging for cerebral blood flow) and peripheral nerve conduction studies. Cardiac uptake of 123I-metaiodobenzylguanidine (MIBG) scintigraphy decreased, with heart to mediastinum (H/M) ratio at 1.73 (examined at 15 min after injection, normal H/M > 1.92). The R–R interval variation on the electrocardiogram was 0.62% at rest. Tonic pupil responded to

\* Corresponding author. Tel.: +81 75 751 3768.

E-mail address: [haruhisa@kuhp.kyoto-u.ac.jp](mailto:haruhisa@kuhp.kyoto-u.ac.jp) (H. Inoue).

0.125% pilocarpine (2/2 mm), establishing denervation hypersensitivity of the pupillary constrictor. At first, because all of the autonomic dysfunctions were localized to postganglionic autonomic nerves, we diagnosed this patient with pure autonomic failure (PAF).

However further laboratory investigation revealed that anti SS-B (La) antibody was positive at 21.7 U/ml (normal <15). Oral and conjunctival sicca were objectively confirmed either by Schirmer test or by Gum test. Salivary gland biopsy revealed lymphocytic infiltration at both periglandular and perivascular regions. All of these sicca findings fulfilled diagnostic criteria of primary SS (Vitali et al., 2002). Moreover, ganglionic AChR antibody was mildly elevated at 300 pmol/l (normal <50 pmol/L). There were no abnormal findings in both tumor markers (including CEA, CA19-9, NSE, SCC, PSA and sIL-2R) and in CT scans from neck to abdomen. Based on these findings, we diagnosed this patient as AAG concomitant with primary SS.

We attempted to administer 1 mg/kg/day prednisolone and gradually tapered to 0.3 mg/kg/day across 3 months. 3 weeks after starting therapy we observed improvement of autonomic dysfunction including orthostatic hypotension, tonic pupil, urinary frequency (returned to normal, less than 2 times a night), constipation and sicca symptoms. Also serum titer of both ganglionic AChR antibody and anti SS-B (La) antibody decreased from 300 to 150 pmol/l and 21.7 to 14.2 U/ml, respectively. After 2 years follow-up we did not observe any symptomatic exacerbation despite prednisolone dosage reduction down to 0.075 mg/kg/day.

## 2.2. Patient 2

A 79-year-old healthy woman presented with oral sicca symptoms for 4 years and also suffered from chronically progressive orthostatic dizziness, which sometimes resulted in faintness. Physiological evaluation revealed orthostatic hypotension (supine position; blood pressure 156/104 mmHg and heart rate 81/min, standing position; 84/52 mmHg and 84/min), tonic pupil (3/3 mm), dry mouth, dry skin of whole body, urinary frequency (more than 6 times a night) and constipation. There were no other abnormal findings on neurologic examination. Routine laboratory examinations of blood, CSF, and urine revealed no abnormal findings. Anti muscarinic acetylcholine receptor M3 antibody was not examined. Plasma noradrenalin concentration decreased to 136 pg/ml (normal 140–570) at rest and failed to respond to tilting. There were no conspicuous abnormalities in MRI and IMP-SPECT and nerve conduction studies. Cardiac uptake of <sup>123</sup>I-MIBG scintigraphy was decreased, with heart to mediastinum (H/M) ratio at 1.40 (examined at 15 min after injection). The R-R interval variation on the electrocardiogram was 1.01% at rest. Tonic pupil responded to 0.125% pilocarpine (2/2 mm), indicating denervation hypersensitivity of the pupillary constrictor.

Anti SS-A (La) antibody was positive, 75.5 U/ml (normal <10). Oral and conjunctival sicca were objectively confirmed by Schirmer test and Gum test. Salivary gland biopsy revealed lymphocytic infiltration at both periglandular and perivascular regions. All of these findings fulfilled diagnostic criteria of primary SS. There were no abnormal findings in both tumor markers (including CEA, CA19-9, NSE, SCC, PSA and sIL-2R) and in CT scans from neck to abdomen. In contrast to patient 1, serum ganglionic AChR antibody was negative in patient 2. Finally we diagnosed her with PAF, partially overlapping with autoimmune autonomic neuropathy (AAN) associated with primary SS.

We attempted to administer 1 mg/kg/day prednisolone and gradually tapered to 0.4 mg/kg/day across 6 months, with no discernible effect on autonomic dysfunction (titer of anti SS-A (La) antibody decreased to 45.5).

## 3. Discussion

In patient 1 we could treat the patient of AAG by oral prednisolone monotherapy. There are no controlled studies of AAG treatment and only a few case reports describe the effectiveness of intravenous

immunoglobulin, plasmapheresis, L-threo-3,4-dihydroxyphenyl-serine (L-threo-DOPS) and a combination of these therapies (Christopher et al., 2008; Modoni et al., 2007; Schroeder et al., 2005). It is difficult to discriminate AAG from AAN or PAF because all of these diseases impair postganglionic autonomic nerves and present similar symptoms. Therefore ganglionic AChR antibody is critical for the diagnosis of AAG, which is treatable by medication.

Patient 1 showed decrease of cardiac MIBG-uptake, indicating postganglionic sympathetic denervation. On the other hand, some cases with AAG showed normal sympathetic innervation, assessed by 6-<sup>18</sup>F fluorodopamine positron emission tomographic scanning (Goldstein et al., 2002). We speculated that the denervation of the present case was derived from secondary impairment of postganglionic nerves by ganglionic AChR antibody or by overlap of SS-induced AAN. Peripheral nerve conduction studies revealed intactness of large fibers in the present cases. However lack of nerve biopsy limited pathological evaluation of peripheral nerves, frequently involved in SS. Therefore we could not exclude the possibilities that different steroid-responses of the present two cases originated from 1) different severity of coincident SS-associated polyneuropathy, or 2) different severity of dysfunction in the autonomic ganglion. Unfortunately we have no modality to determine the histopathological distribution among autonomic ganglia, postganglionic nerve fibers, or both. Consequently the term 'ganglioneuropathy' can be more appropriate for cases like patient 1. Furthermore, urinary urgency, observed in the present two cases, is an unusual finding for AAN. We speculate that this urinary urgency was partially caused by Sjögren syndrome and the anti muscarinic acetylcholine receptor M3 antibody (Wang et al., 2004).

SS is a systemic autoimmune disease characterized by sicca symptoms, and accompanied by a wide variety of neurological complications. Among these, AAN is a rare complication of SS (Mori et al., 2005). AAN originating from SS is usually refractory to immunomodulative therapy (Shimoyama et al., 2002). Patient 1 (with primary SS and mildly elevated ganglionic AChR antibody) showed marked response to oral prednisolone, even though patient 2 (with SS and without ganglionic AChR antibody) was refractory to oral prednisolone. In primary SS, not only cellular immunity but also humoral immunity plays an important role. Primary SS is currently recognized as a multifactorial disorder associated with various antibodies (e.g. anti SS-A/Ro antibody, anti SS-B/La antibody, anti alpha-fodrin antibody, anti muscarinic acetylcholine receptor antibody etc.). Our cases suggest that a part of AAG may be relevant to SS and treatable by immunomodulatory therapy. However our present report is based on a limited number of cases and case accumulation is necessary to clarify the precise association between AAG and SS.

## Acknowledgement

The authors wish to thank Dr Gavinio R. for editing the manuscript.

## References

- Christopher, H., Gibbons, C.H., Vernino, S.A., Freeman, R., 2008. Combined immunomodulatory therapy in autoimmune autonomic ganglionopathy. *Arch. Neurol.* 65, 213–217.
- Goldstein, D.S., Holmes, C., Dendi, R., Li, S.T., Brentzel, S., Vernino, S., 2002. Pandsyautonomia associated with impaired ganglionic neurotransmission and circulating antibody to the neuronal nicotinic receptor. *Clin. Auton. Res.* 12, 281–285.
- Low, P.A., Vernino, S., Suarez, G., 2003. Autonomic dysfunction in peripheral nerve disease. *Muscle Nerve* 27, 646–661.
- Modoni, A., Mirabella, M., Madia, F., Sanna, T., Lanza, G., Tonali, P.A., Silvestri, G., 2007. Chronic autoimmune autonomic neuropathy responsive to immunosuppressive therapy. *Neurology* 68, 161–162.
- Mori, K., Iijima, M., Koike, H., Hattori, N., Tanaka, F., Watanabe, H., Katsuno, M., Fujita, A., Aiba, I., Ogata, A., Saito, T., Asakura, K., Yoshida, M., Hirayama, M., Sobue, G., 2005. The wide spectrum of clinical manifestations in Sjögren's syndrome-associated neuropathy. *Brain* 128, 2518–2534.
- Schroeder, C., Vernino, S., Birkenfeld, A.L., Tank, J., Heusser, K., Lipp, A., Benter, T., Lindschau, C., Ketritz, R., Luft, F.C., Jordan, J., 2005. Plasma exchange for primary autoimmune autonomic failure. *N. Engl. J. Med.* 353, 1585–1590.

- Shimoyama, M., Ohtahara, A., Okamura, T., Watanabe, M., Fujimoto, Y., Teshima, S., Takeda, S., Hisatome, I., Shigamasa, C., 2002. Isolated autonomic cardiovascular neuropathy in a patient with primary Sjögren syndrome: a case of successful treatment with glucocorticoid. *Am. J. Med. Sci.* 324, 170–172.
- Vernino, S., Low, P.A., Fealey, R.D., Stewart, J.D., Farrugia, G., Lennon, V.A., 2000. Autoantibodies to ganglionic acetylcholine receptors in autoimmune autonomic neuropathies. *N. Engl. J. Med.* 343, 847–855.
- Vitali, C., Bombardieri, S., Jonsson, R., Moutsopoulos, H.M., Alexander, E.L., Carsons, S.E., Daniels, T.E., Fox, P.C., Fox, R.I., Kassan, S.S., Pillemer, S.R., Talal, N., Weisman, M.H., European Study Group on Classification Criteria for Sjögren's Syndrome, 2002. Classification criteria for Sjögren's syndrome: a revised version of the European criteria proposed by the American–European Consensus Group. *Ann. Rheum. Dis.* 61, 554–558.
- Wang, F., Jackson, M.W., Maughan, V., Cavill, D., Smith, A.J., Waterman, S.A., Gordon, T.P., 2004. Passive transfer of Sjögren's syndrome IgG produces the pathophysiology of overactive bladder. *Arthritis Rheum.* 50, 3637–3645.



## Diagnostic accuracy of cardiac metaiodobenzylguanidine scintigraphy in Parkinson disease

H. Sawada<sup>a,b</sup>, T. Oeda<sup>a,b</sup>, K. Yamamoto<sup>a,b</sup>, N. Kitagawa<sup>a,b</sup>, E. Mizuta<sup>a,b</sup>, R. Hosokawa<sup>c</sup>, M. Ohba<sup>c</sup>, R. Nishio<sup>c</sup>, K. Yamakawa<sup>a,d</sup>, H. Takeuchi<sup>a,d</sup>, S. Shimohama<sup>d</sup>, R. Takahashi<sup>d</sup> and T. Kawamura<sup>e,1</sup>

<sup>a</sup>Clinical Research Center, Utano National Hospital, Kyoto, Japan; <sup>b</sup>Center for Parkinson Disease and Related Disorders, Utano National Hospital, Kyoto, Japan; <sup>c</sup>Department of Cardiology, Kyoto University Hospital, Kyoto, Japan; <sup>d</sup>Department of Neurology, Kyoto University Hospital, Kyoto, Japan; and <sup>e</sup>Kyoto University Health Service, Kyoto, Japan

### Keywords:

norepinephrine, preclinical diagnosis, ROC curve, sympathetic nerve

Received 16 August 2008

Accepted 17 October 2008

**Background and purpose:** To estimate the diagnostic accuracy of cardiac <sup>123</sup>I-metaiodobenzylguanidine (MIBG) scintigram for detection of Parkinson disease. **Methods:** A cross-sectional study with index test of MIBG scintigram and reference standard of U.K. Parkinson's Disease Brain Bank Criteria was performed in 403 patients. Ratio of cardiac-to-mediastinum MIBG accumulation was determined at 20 min (early H/M) and 4 h (late H/M). Area under the receiver-operator characteristic (ROC) curve, sensitivity and specificity in detecting Parkinson disease were analyzed. Accuracy was analyzed in a subgroup of patients with disease duration of 3 years or less. **Results:** Area under the ROC curve was 0.89 using either early or late H/M as a diagnostic marker (95% CI 0.85–0.92 for early H/M and 0.86–0.93 for late H/M). Sensitivity and specificity were 81.3% (76.1–85.8%) and 85.0% (77.7–90.6%) for early H/M and 84.3% (79.3–88.4%) and 89.5% (83.01–94.1%) for late H/M. In the subgroup with duration of 3 years or less, the ROC curve area, sensitivity, and specificity were 0.86 (0.79–0.92), 76.0% (64.8–85.1%), and 83.9% (71.7–92.4%) for early H/M and 0.85 (0.78–0.92), 73.3% (61.9–82.9%), and 87.5% (75.9–94.8%) for late H/M. **Conclusion:** Although diagnostic accuracy of cardiac MIBG scintigram is high, it is limited because of insufficient sensitivity in patients with short duration.

### Introduction

In Parkinson disease degeneration of striatal dopaminergic neuronal terminals can be detected by neuroimaging using carbomethoxy-iodophenyl-tropane [1,2], or fluorodopa [3]. However, these findings are not disease specific because they may be observed in multiple system atrophy and progressive supranuclear palsy [4].

Sympathetic post-ganglionic fibers are markedly lost in the myocardium of patients with Parkinson disease [5–7], and denervation precedes the neuronal loss in the sympathetic ganglion [8] and the extent reflects pathological changes in sympathetic ganglion cells [5].

Goldstein and colleagues demonstrate that sympathetic neurocirculatory failure is important feature for the disease [9,10]. Denervation of cardiac sympathetic nerve terminals have been proven by a study using 6-<sup>18</sup>F-fluorodopamine [9] and is thought to be specific

for Parkinson disease [10–13]. Additionally, studies have revealed that uptake of metaiodobenzylguanidine (MIBG) into the myocardium is reduced in patients with Parkinson disease [12,14,15]. Cardiac sympathetic denervation can precede motor disturbance [16], and might be marked even in the initial stage of Parkinson disease [15]. However, it remains to be determined whether a reduction in cardiac MIBG accumulation is sensitive and specific enough to detect Parkinson disease, especially in the disease's early stages [17].

### Subjects and methods

#### Study subjects

We enrolled 403 consecutive patients with muscular rigidity, hand or leg tremor, or slowed movements who had undergone a <sup>123</sup>I-MIBG cardiac scintigram at the two hospitals. Patients with history of myocardial infarction, current heart diseases including heart failure and cardiomyopathy, uncontrolled diabetes mellitus, and current use of tricyclic antidepressants or selegiline (10 mg or more) were excluded because tricyclic antidepressants block MIBG uptake and selegiline

Correspondence: Dr Hideyuki Sawada, Clinical Research Center, Utano National Hospital, 8 Ondoyamacho, Ukyoku, Kyoto, Japan (tel.: +81-75-461-5121; fax: +81-75-464-0021; e-mail: sawada@unh.hosp.go.jp).

<sup>1</sup>Statistical analysis was conducted by Takashi Kawamura.

elevates serum norepinephrine concentrations. Informed consent was obtained from the participants. A total of 413 tests were performed in 403 patients, and 10 of these patients received an MIBG test at both hospitals.

#### Reference standard for clinical diagnosis of Parkinson disease

A detailed history was taken and neurological examinations were performed to make a clinical diagnosis of Parkinson disease according to the United Kingdom Parkinson's Disease Society Brain Bank Clinical Diagnostic Criteria (UK PD Brain Bank Criteria) [18]. These criteria were used as the reference standard, blind to the results of MIBG tests. Parkinson disease was diagnosed after fulfilling steps 1, 2 and 3 of UK PD Brain Bank criteria. Brain magnetic resonance imaging (MRI) was used to confirm the diagnosis of Parkinson disease.

#### Protocol for cardiac scintigram of MIBG

To investigate cardiac sympathetic nerve terminal denervation, 3 mCi (111 MBq)  $^{123}\text{I}$ -MIBG was injected intravenously into each patient in the supine position. A planar image of the chest was obtained at 20 min and at 4 h. The regions of interest were set in the heart, mediastinum, and lung. Relative cardiac accumulation was calculated as the ratio of the heart to the mediastinum at 20 min (early H/M) and at 4 h (late H/M).

#### Interhospital reliability

Interhospital reliability was assessed by agreement of H/M using the method of Bland and colleagues [19] in patients who had been tested at both hospitals. The relative ratio of the H/M values of the tests performed at the two hospitals was plotted. The latest H/M values of these 10 patients are incorporated into the analysis for the area under ROC curves, sensitivity and specificity.

#### Relationship between cardiac MIBG uptake and the severity and duration of Parkinson disease

Because some patients have 'wearing-off' or 'on-off' phenomena we evaluated the severity of such patients in the 'on' period. Patients were assigned to five groups according to the Hoehn and Yahr Stage (H-Y), and the relationship between the grades on the H-Y and H/M was analyzed. We analyzed the relationship between the Unified Parkinson's Disease Rating Scale subset-3 (UPDRS-3) or disease duration and H/M in patients with Parkinson disease.

#### Determination of a cut-off point of H/M as a diagnostic marker and diagnostic accuracy

According to the ROC curve, we determined the most discriminative cut-off point of H/M for diagnosing Parkinson disease. The positive likelihood ratio, or a ratio of true-positive to false-positive, was calculated at the cut-off point. The negative likelihood ratio also was determined. To evaluate the diagnostic accuracy of the MIBG test in the early stages of the disease, we classified patients into two subgroups, those with disease duration of 3 years or less and those with disease duration longer than 3 years. We investigated the statistical diagnostic accuracy in these two subgroups.

#### Statistical analysis

Sample size was determined by power analysis comparing two means. According to our previous study, we estimated the mean H/M to be  $2.45 \pm 0.47$  (mean  $\pm$  SD) in control patients [20]. We hypothesized that H/M should be lower in Parkinson disease than in other disorders and that the MIBG test should detect the difference of 0.1 of H/M. The sample size was calculated as 398 for a power greater than 80% and an  $\alpha$  error of 0.05, one-sided test.

Owing to its non-Gaussian distribution, the difference in H/M in the groups of patients with Parkinson disease and with other disorders was statistically analyzed using the non-parametric Mann-Whitney *U* test. The correlation between H/M and the severity (H-Y grades or UPDRS-3 scores) or duration of the illness was analyzed using the non-parametric Spearman's rank correlation test. All statistical analyses were carried out using GraphPad Prism 4.0 for Windows (GraphPad Software, San Diego, CA, USA, <http://www.graphpad.com>). Data were expressed as mean  $\pm$  SD. *P* values less than 0.05 were considered statistically significant.

## Results

#### Subjects characteristics

Excluding three patients (one because of cardiomyopathy and two because they had been prescribed selegiline 10 mg), 400 patients were included in the study. Of these, 267 were diagnosed as having Parkinson disease according to the UK PD Brain Bank Clinical Diagnostic Criteria. According to the UK PD Brain Bank Criteria, patients with severe disturbance of cognition in the early phase were not included in those having Parkinson disease, but patients presenting with

mild-to-moderate cognitive disturbances were included. Thirty-three patients showed clinical features suggesting Lewy body disease, and they were included in Parkinson disease because they fulfilled the criteria for Parkinson disease. Additionally, no abnormal MRI findings suggested multiple system atrophy in any of the 267 patients. Of the remaining 133 patients who did not fulfill the criteria for Parkinson disease, 76 had features typical of diseases other than Parkinson; these persons had multiple system atrophy ( $n = 36$ ), progressive supranuclear palsy ( $n = 15$ ), essential tremor ( $n = 12$ ), Alzheimer's disease with extrapyramidal signs ( $n = 5$ ), corticobasal degeneration ( $n = 3$ ), stroke ( $n = 3$ ), drug-induced Parkinsonism ( $n = 1$ ), and motor neuron disease with extrapyramidal signs ( $n = 1$ ) (Fig. 1). The remaining 57 patients had extrapyramidal signs but were not given a specific clinical diagnosis. We accepted all of these 133 patients as not having Parkinson disease (Table 1).

### Interhospital reliability

Interhospital agreement of the MIBG was evaluated in 10 patients (eight with Parkinson disease and two with progressive supranuclear palsy). The intervals of the tests in the two hospitals were 8 months to 3 years. The interhospital agreement was a mean bias of 1.03 with limits of agreement of 0.87–1.22 (95% CI) for early H/M and a mean bias of 1.08 with limits of agreement of 0.78–1.50 (95% CI) for late H/M. Agreement of the tests was higher in early H/M than in late H/M (Fig. 2).

### Relationship between cardiac MIBG uptake and the severity and duration of Parkinson disease

Cardiac accumulation of MIBG was significantly reduced in patients with Parkinson disease compared with those without Parkinson disease (Fig. 3). The mean early H/M value was  $2.39 \pm 0.49$  in patients with other

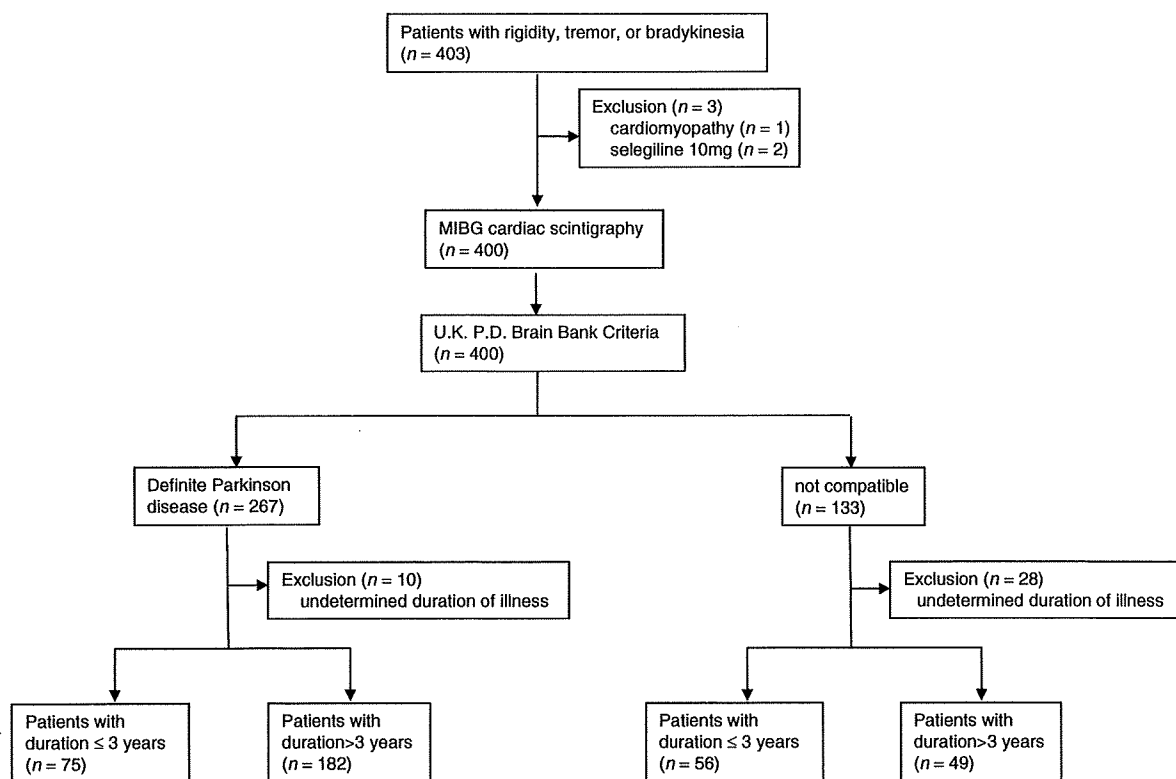


**Figure 1** Flow diagram of the eligible patients and the enrolling process of the study. Eligible patients were 403 consecutive patients who underwent MIBG cardiac scintigraphy because of extrapyramidal signs; three patients were excluded: one with cardiomyopathy and one using selegiline (10 mg); this left 400 enrolled patients. According to the UK Brain Bank criteria of Parkinson's disease as a reference standard, 267 of 400 patients had Parkinson disease, and the remaining 133 patients had other disorders. Diagnostic accuracy was analyzed in 400 patients. Of the 267 patients with Parkinson disease, 10 with unspecified disease duration were excluded. Of the 133 patients without Parkinson disease, 28 with unspecified disease duration were excluded. The remaining patients were separated into two groups: those with a disease duration of 3 years or less (75 patients with Parkinson disease and 56 patients without Parkinson disease) and those with a disease duration longer than 3 years (56 patients with Parkinson disease and 49 patients without Parkinson disease).

Table 1 Patient characteristics

	<i>n</i>	M/F	Age [Mean (SD)]
Parkinson disease	267	116/151	70.1 (10.0)
Other disorders without Parkinson disease	133	76/57	70.4 (8.7)

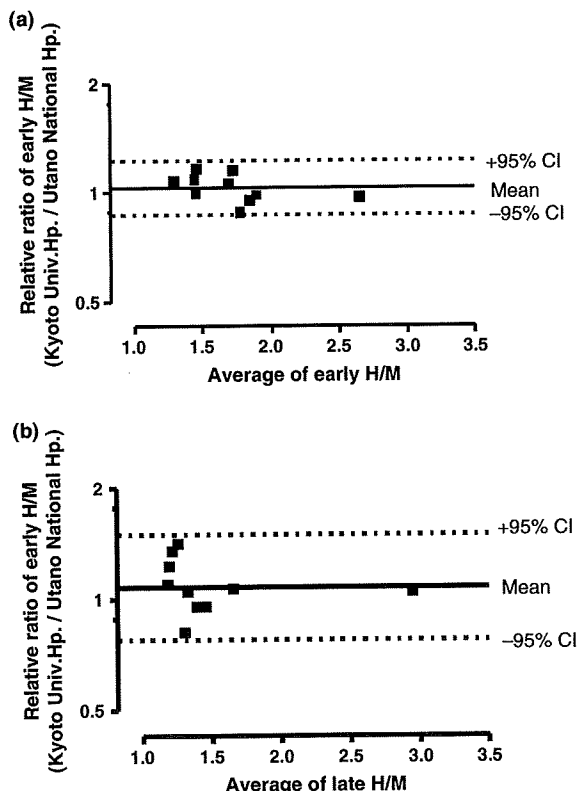


Figure 2 Bland-Altman plots for interhospital agreement of early H/M (a) and late H/M (b). The vertical axis represents the ratio of H/M performed at Kyoto University Hospital to those performed at Utano National Hospital. The bias was expected to be 1.0 when there is complete interhospital agreement.

disorders and  $1.66 \pm 0.33$  in patients with Parkinson disease; this difference was highly significant ( $P < 0.001$ ). Similarly, the mean late H/M value of  $1.44 \pm 0.39$  in patients with Parkinson disease was significantly lower than that for patients with other extrapyramidal disorders ( $2.42 \pm 0.62$ ;  $P < 0.001$ ).

According to the H-Y grades, 267 patients with Parkinson disease were separated into five groups: H-Y 1 ( $n = 12$ ), H-Y 2 ( $n = 49$ ), H-Y 3 ( $n = 74$ ), H-Y 4 ( $n = 96$ ), and H-Y 5 ( $n = 18$ ). Eighteen patients were excluded from the subgroup analysis because the H-Y grade could not be specified. The relationship

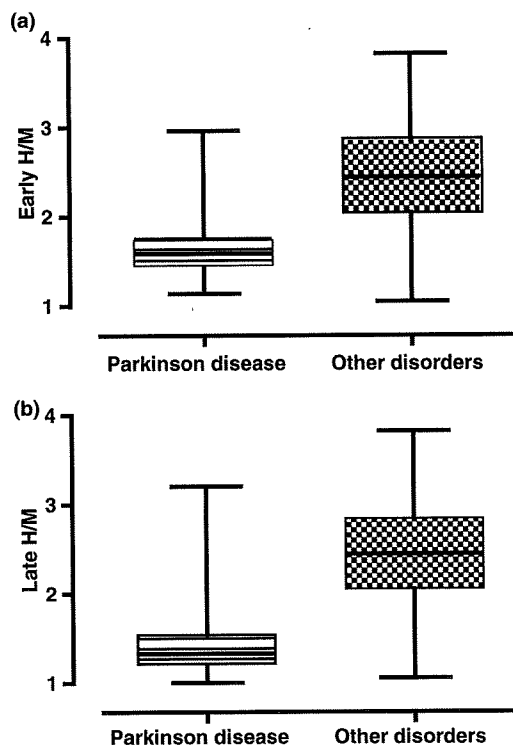
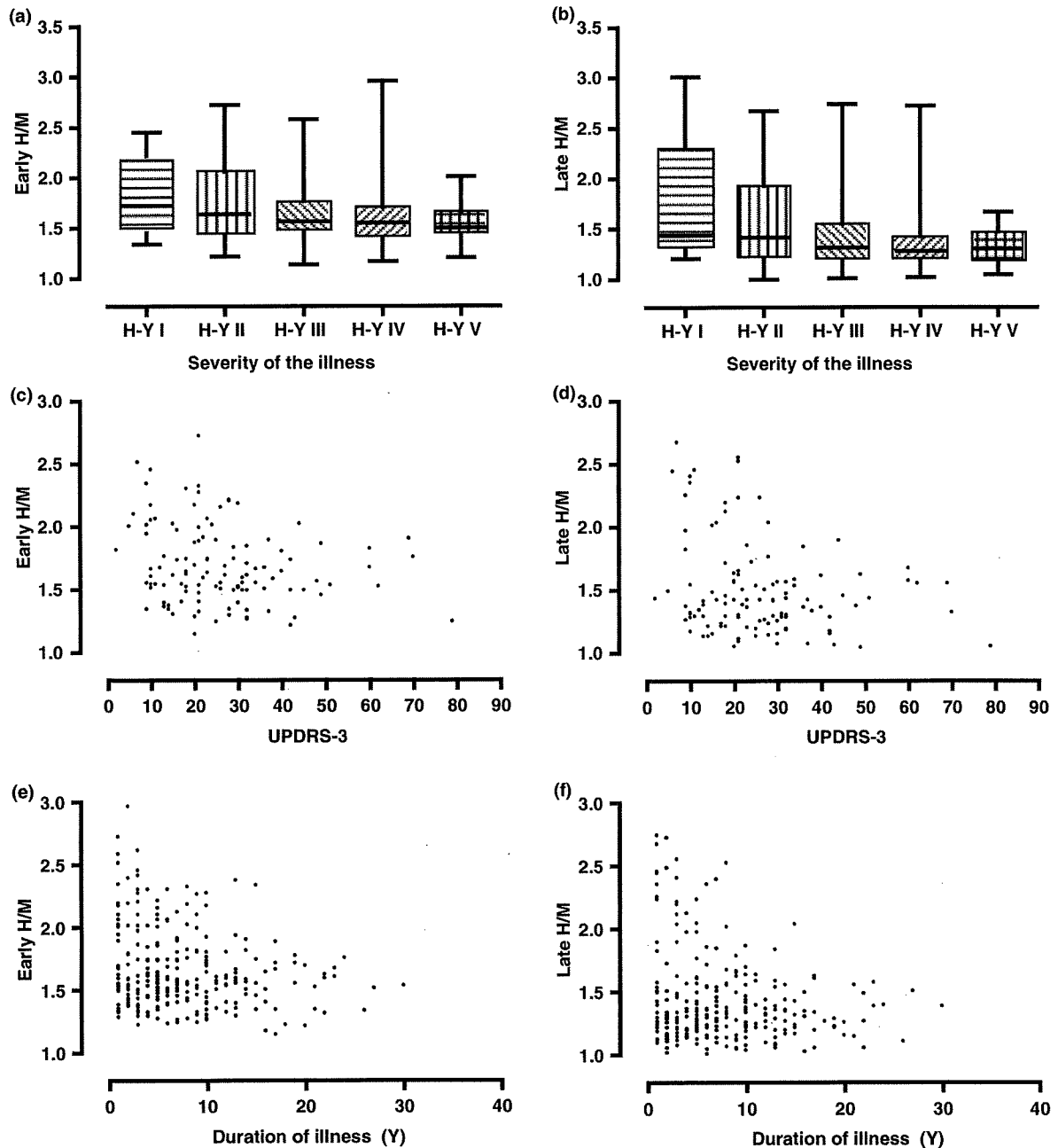


Figure 3 Box plot with whiskers presenting early H/M (a) and late H/M of patients with Parkinson disease and those with other disorders. Early and late H/M was significantly lower in patients with Parkinson disease than it was in patients with other disorders. Box shoulders represent the 25th and 75th percentiles of the distribution and whiskers represent minimum and maximum data of the groups. The difference in H/M was significant between patients with Parkinson disease and those with other disorders.

between H-Y grades and H/M was analyzed in the remaining 249 patients (Fig. 4a and b). There was a significant negative correlation between early H/M and H-Y grade (Spearman  $r = -0.184$ ,  $P = 0.0036$ ). Similarly, late H/M also was negatively correlated with H-Y grade ( $r = -0.23$ ,  $P = 0.0004$ ). The relationship between UPDRS-3 score and H/M was analyzed in 116 patients whose UPDRS-3 scores were obtained. There was a significant negative correlation between late H/M and UPDRS-3 scores [ $r = -0.215$ ,  $P = 0.0204$  (early H/M) and  $r = -0.231$ ,  $P = 0.013$  (late H/M)] (Fig. 4c and d). In addition, the relationship between the duration of the illness and H/M was analyzed in 257 patients. Ten patients were excluded from this analysis because the duration of their illness had not been determined. Early and late H/M reduction correlated significantly with the duration of illness ( $r = -0.1548$ ,  $P = 0.013$  for early H/M,  $r = -0.1379$ ,  $P = 0.027$  for late H/M) (Fig. 4e and f).



**Figure 4** Relationship of H/M to the severity and duration of Parkinson disease. Early and late H/M decreased with both the Hoehn-Yahr grades (range, 1–5; 1 = unilateral disability, 5 = bed- or wheelchair-bound) (a, b) and UPDRS-3 scores (semiquantitative scale of motor disturbance of unified Parkinson’s disease rating scale, range, 0–108, 0 = best, 108 = worst) (c, d). Furthermore, H/M decreased in parallel with the duration of the illness (e, f).

**Determination of a cut-off point of H/M as a diagnostic marker**

The area under the ROC curve was 0.89 (95% CI, 0.85–0.92) for early H/M and 0.89 (0.86–0.93) for late H/M. According to the ROC curves, the most discriminative

cut-off point was 1.92 for early H/M and 1.68 for late H/M (Fig. 5). The sensitivity and specificity was 81.3% (95% CI, 76.1–85.8%) and 85.0% (77.7–90.6%) for early H/M (<1.92) and 84.3% (79.3–88.4%) and 89.5% (83.0–94.1%) for late H/M (<1.68). At these cut-off points, the positive likelihood ratio was 5.40

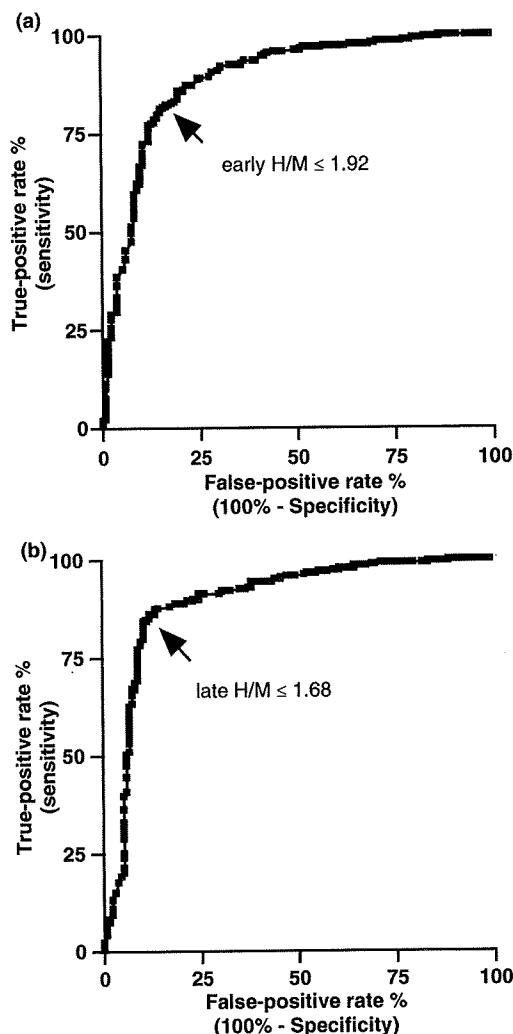


Figure 5 Curves of receiver-operator characteristics (ROC) of the diagnosis of Parkinson disease in early H/M (a) and late H/M (b). The most discriminative cut-off point (near the left upper corner of the graph) is represented by arrows. The sensitivity and specificity were determined according to the ROC curves.

(2.71–10.8) for early H/M and 8.01 (2.84–22.6) for late H/M. The negative likelihood ratio was 0.22 (0.15–0.33) for early H/M and 0.18 (0.11–0.29) for late H/M. The diagnostic accord between MIBG criteria and UK PD brain bank diagnostic criteria is shown in Table 2.

**Analysis in patients with short and long duration**

According to disease duration, 362 patients were classified into two subgroups: 131 patients with disease duration of 3 years or less and 231 patients with disease duration more than 3 years. Seventy-five of the 131 patients and 182 of the 231 patients, respectively, were

Table 2 Contingency table for diagnosis of Parkinson disease

Patients category	MIBG test	UK brain bank criteria	
		PD	non-PD
Total	Early H/M		
	+	217	20
	-	50	113
	Late H/M		
Duration ≤ 3 years	+	225	14
	-	42	119
	Early H/M		
	+	57	9
Duration > 3 years	-	18	47
	Late H/M		
	+	55	7
	-	20	49
Duration > 3 years	Early H/M		
	+	152	5
	-	30	44
	Late H/M		
Duration > 3 years	+	164	5
	-	18	44

diagnosed with Parkinson disease according to the UK PD brain bank criteria. Thirty-eight patients (10 with Parkinson disease and 28 with other disorders) were excluded from the subgroup analysis because of an undetermined onset of the extrapyramidal signs (Fig. 1). ROC curves were obtained, and these curves were used to determine the most discriminative cut-off points for diagnosing Parkinson disease in the subgroups (Fig. 6).

Analyses of the subgroup of patients with duration of 3 years or less led to an area under the ROC curve of 0.86 (0.79–0.92) for early H/M and 0.85 (0.78–0.92) for late H/M. According to the ROC curves, the most discriminative cut-off points were 2.04 for early H/M and 1.84 for late H/M. For early H/M, the sensitivity and specificity were 76.0% (64.8–85.1%) and 83.9% (71.7–92.4%). For late H/M, the sensitivity and specificity were 73.3% (61.9–82.9%) and 87.5% (75.9–94.8%). Positive likelihood ratios were 4.73 for early H/M and 5.87 for late H/M.

Analyses of the subgroup of patients with duration longer than 3 years led to an area under the ROC curve of 0.91 (0.86–0.96) for early H/M and 0.92 (0.86–0.98) for late H/M. The sensitivity and specificity were 83.5% (77.3–88.6%) and 89.8% (77.8–96.6%) (early H/M < 1.83) or 90.1% (84.8–94.0%) and 89.8% (77.8–96.6%) (late H/M < 1.68). Positive likelihood ratios were 8.19 for early H/M and 8.83 for late H/M. The relationship of MIBG test results and UK PD brain bank criteria is shown in Table 2, and the accuracy of the MIBG test in diagnosing Parkinson disease is summarized in Table 3.

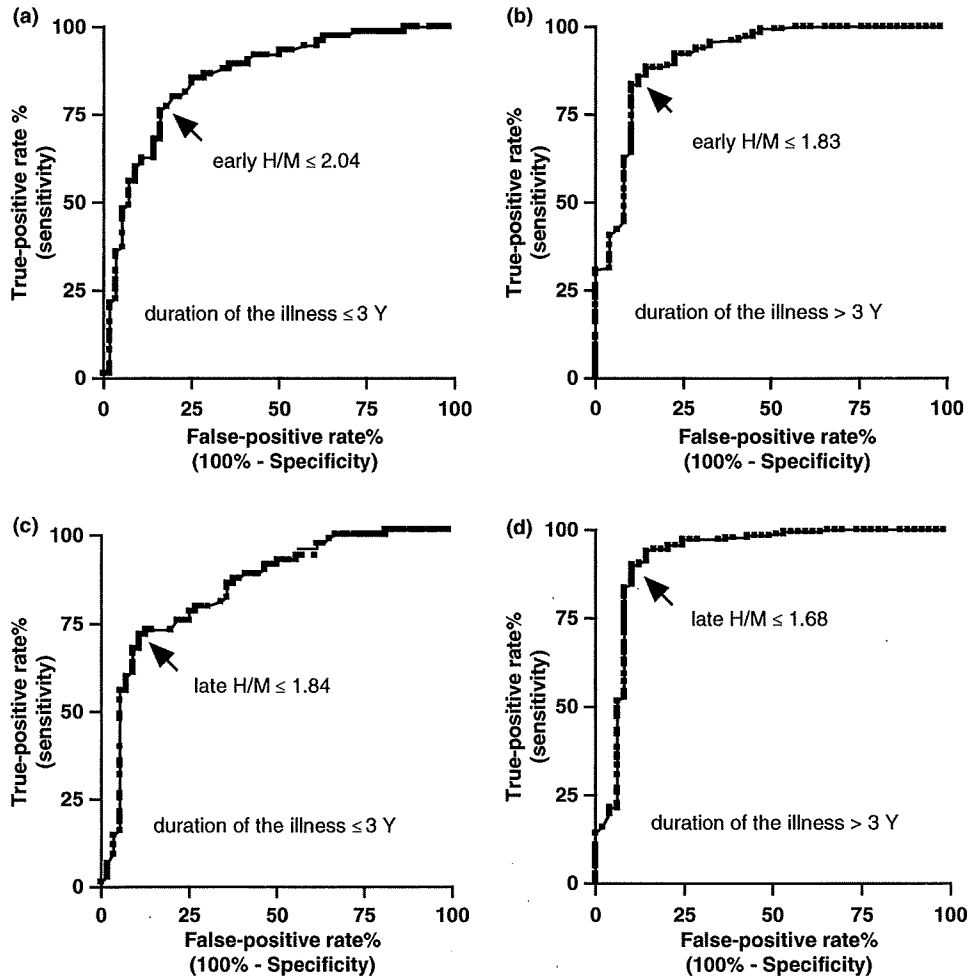


**Figure 6** ROC curves in patients with shorter and longer durations of illness. ROC curves were created in a subgroup of patients with disease duration of 3 years or less (a, c) and with disease duration longer than 3 years (b, d). Recruitment of the subjects is demonstrated in Fig. 1b. The most discriminative cut-off points were set nearest to the upper left corner of the graph (arrows).

**Table 3** Diagnostic accuracy of MIBG test in diagnosis of Parkinson disease

	Early H/M			Late H/M		
	Duration ≤ 3 years	Duration > 3 years	Total	Duration ≤ 3 years	Duration > 3 years	Total
AUC of ROC	0.86 (0.79–0.92)	0.91 (0.86–0.97)	0.89 (0.85–0.92)	0.85 (0.78–0.92)	0.92 (0.86–0.98)	0.89 (0.86–0.93)
Most discriminative cut-off point	2.04	1.83	1.92	1.84	1.68	1.68
Sensitivity, %	76.0 (64.8–85.1)	83.5 (77.3–88.6)	81.3 (76.1–85.8)	73.3 (61.9–82.9)	90.1 (84.8–94.0)	84.3 (79.3–88.4)
Specificity, %	83.9 (71.7–92.4)	89.8 (77.8–96.6)	85.0 (77.7–90.6)	87.5 (75.9–94.8)	89.8 (77.8–96.6)	89.5 (83.0–94.1)
Positive likelihood ratio	4.73 (1.83–12.2)	8.19 (1.42–47.2)	5.40 (2.71–10.8)	5.87 (1.68–20.5)	8.83 (1.44–54.1)	8.00 (2.84–22.6)
Negative likelihood ratio	0.29 (0.17–0.48)	0.18 (0.10–0.33)	0.22 (0.15–0.33)	0.30 (0.19–0.48)	0.11 (0.04–0.30)	0.18 (0.11–0.29)

Parenthesis indicates 95% confidential intervals.

**Discussion**

Consistent with previous studies, cardiac accumulation of MIBG has been shown to be significantly reduced in

patients with Parkinson disease [10,12,14,15]. In previous studies, it has been controversial whether reduction in H/M is associated with the severity and duration of the illness [1,11,21], and the controversy could depend

on the size of the study sample. In the current study, a reduction in H/M was mildly but significantly associated with the severity and duration of the illness. Orimo and colleagues demonstrated that a reduction in cardiac MIBG accumulation reflects the degeneration of post-ganglionic sympathetic nerve terminals in the myocardium [8]. In addition to sporadic patients, cardiac uptake of  $^{18}\text{F}$ -fluorodopamine is also reduced in patients with a mutation or triplication of the  $\alpha$ -synuclein gene [22], which causes familial Parkinson disease with autosomal dominant inheritance [23]. In this context, a reduction in MIBG cardiac accumulation reflects the systemic pathological process of the disease and may be a peripheral biological marker of Parkinson disease including triplication of the  $\alpha$ -synuclein gene.

The diagnostic accuracy of index test is limited by that of standard reference test and it was not confirmed pathologically in this study. In addition to this limitation the following several points can be limitation of the study. In contrast to  $\alpha$ -synuclein gene triplication, MIBG cardiac accumulation is preserved in patients with mutations in the Park2 gene [24] and they may be diagnosed with definite Parkinson disease according to UK PD brain bank criteria. A recent study suggests that cardiac MIBG accumulation is often preserved in patients with hereditary Parkinsonism including LRRK2 [25]. According to the UK PD brain bank criteria patients with autosomal dominant hereditary Parkinsonism may not be diagnosed as Parkinson disease because patients with two or more members who are diagnosed as the disease are excluded. Additionally, cardiac accumulation of MIBG may be preserved in an early stage of Parkinson disease as shown in Fig. 4. Therefore, patients with Park2 mutations or those in the early stages of Parkinson disease may show false-negative results on the MIBG test. There were no specific neurological features in patients with preserved MIBG uptake who were diagnosed as Parkinson disease.

In a Bland-Altman plot, the mean interhospital bias of H/M was small (1.03 for early H/M and 1.08 for late H/M, complete agreement was expected when the bias was calculated as 1.0), but the range of limits was relatively wide. The interhospital concordance might have been influenced by the intervals of the tests because cardiac MIBG uptake can decrease during the course of Parkinson disease [26]. In the context of temporal influences, interhospital reliability may be accepted clinically as an objective diagnostic marker especially in early H/M.

As shown in Fig. 4e and f, H/M was preserved above 2.0 in some patients with a short duration of Parkinson disease. In patients with a disease duration of 10 years or more, late H/M was lower than 2.2 without excep-

tion. These results suggest the possibility that peripheral sympathetic denervation succeeds or precedes degeneration of striatal dopaminergic nerve terminals. In the subgroup of patients with a disease duration of 3 years or less, the sensitivity was low; however, the positive likelihood ratio, area under the ROC curve, and specificity were high enough to make a diagnosis.

### Acknowledgements

We would like to thank Yoshihisa Matsumoto for his technical support with MIBG scintigraphy at Utano National Hospital. We also thank Dr Fukashi Udaka at Sumitomo Hospital, Osaka, Japan for helpful discussion.

### Funding

This work was supported by grants-in-aid for scientific research from the Minister of Health, Labor, and Welfare of Japan and the National Hospital Organization in the management and preparation of the study.

### References

1. Spiegel J, Mollers MO, Jost WH, *et al.* FP-CIT and MIBG scintigraphy in early Parkinson's disease. *Movement Disorders* 2005; **20**: 552–561.
2. Seibyl JP, Marek KL, Quinlan D, *et al.* Decreased single-photon emission computed tomographic [ $^{123}\text{I}$ ]beta-CIT striatal uptake correlates with symptom severity in Parkinson's disease. *Annals of Neurology* 1995; **38**: 589–598.
3. Brooks DJ, Playford ED, Ibanez V, *et al.* Isolated tremor and disruption of the nigrostriatal dopaminergic system: an 18F-dopa PET study. *Neurology* 1992; **42**: 1554–1560.
4. Marshall V, Grosset D. Role of dopamine transporter imaging in routine clinical practice. *Movement Disorders* 2003; **18**: 1415–1423.
5. Mitsui J, Saito Y, Momose T, *et al.* Pathology of the sympathetic nervous system corresponding to the decreased cardiac uptake in 123I-metaiodobenzylguanidine (MIBG) scintigraphy in a patient with Parkinson disease. *Journal of the Neurological Sciences* 2006; **243**: 101–104.
6. Orimo S, Oka T, Miura H, *et al.* Sympathetic cardiac denervation in Parkinson's disease and pure autonomic failure but not in multiple system atrophy. *Journal of Neurology, Neurosurgery and Psychiatry* 2002; **73**: 776–777.
7. Iwanaga K, Wakabayashi K, Yoshimoto M, *et al.* Lewy body-type degeneration in cardiac plexus in Parkinson's and incidental Lewy body diseases. *Neurology* 1999; **52**: 1269–1271.
8. Orimo S, Amino T, Itoh Y, *et al.* Cardiac sympathetic denervation precedes neuronal loss in the sympathetic ganglia in Lewy body disease. *Acta Neuropathologica (Berlin)* 2005; **109**: 583–588.
9. Goldstein DS, Holmes C, Li ST, Bruce S, Metman LV, Cannon RO, 3rd. Cardiac sympathetic denervation in



- Parkinson disease. *Annals of Internal Medicine* 2000; **133**: 338–347.
10. Goldstein DS. Dysautonomia in Parkinson's disease: neurocardiological abnormalities. *Lancet Neurology* 2003; **2**: 669–676.
  11. Nagayama H, Hamamoto M, Ueda M, Nagashima J, Katayama Y. Reliability of MIBG myocardial scintigraphy in the diagnosis of Parkinson's disease. *Journal of Neurology, Neurosurgery and Psychiatry* 2005; **76**: 249–251.
  12. Orimo S, Ozawa E, Nakade S, Sugimoto T, Mizusawa H. (123)I-metaiodobenzylguanidine myocardial scintigraphy in Parkinson's disease. *Journal of Neurology, Neurosurgery and Psychiatry* 1999; **67**: 189–194.
  13. Yoshita M. Cardiac uptake of [123I]MIBG separates PD from multiple system atrophy. *Neurology* 2000; **54**: 1877–1878.
  14. Takatsu H, Nagashima K, Murase M, *et al.* Differentiating Parkinson disease from multiple-system atrophy by measuring cardiac iodine-123 metaiodobenzylguanidine accumulation. *JAMA* 2000; **284**: 44–45.
  15. Druschky A, Hilz MJ, Platsch G, *et al.* Differentiation of Parkinson's disease and multiple system atrophy in early disease stages by means of I-123-MIBG-SPECT. *Journal of the Neurological Sciences* 2000; **175**: 3–12.
  16. Orimo S, Takahashi A, Uchihara T, *et al.* Degeneration of cardiac sympathetic nerve begins in the early disease process of Parkinson's disease. *Brain Pathology* 2007; **17**: 24–30.
  17. Gerlach M, Hendrich A, Hueber R, *et al.* Early detection of Parkinson's disease: unmet needs. *Neuro-Degenerative Diseases* 2008; **5**: 137–139.
  18. Daniel SE, Lees AJ. Parkinson's Disease Society Brain Bank, London: overview and research. *Journal of Neural Transmission. Supplementum* 1993; **39**: 165–172.
  19. Bland JM, Altman DG. Statistical methods for assessing agreement between two methods of clinical measurement. *Lancet* 1986; **1**: 307–310.
  20. Sawada H, Yamakawa K, Yamakado H, *et al.* Cocaine and phenylephrine eye drop test for Parkinson disease. *JAMA* 2005; **293**: 932–934.
  21. Hamada K, Hirayama M, Watanabe H, *et al.* Onset age and severity of motor impairment are associated with reduction of myocardial 123I-MIBG uptake in Parkinson's disease. *Journal of Neurology, Neurosurgery and Psychiatry* 2003; **74**: 423–426.
  22. Singleton A, Gwinn-Hardy K, Sharabi Y, *et al.* Association between cardiac denervation and parkinsonism caused by alpha-synuclein gene triplication. *Brain* 2004; **127**: 768–772.
  23. Singleton AB, Farrer M, Johnson J, *et al.* alpha-Synuclein locus triplication causes Parkinson's disease. *Science* 2003; **302**: 841.
  24. Orimo S, Amino T, Yokochi M, *et al.* Preserved cardiac sympathetic nerve accounts for normal cardiac uptake of MIBG in PARK2. *Movement Disorders* 2005; **20**: 1350–1353.
  25. Quattrone A, Bagnato A, Annesi G, *et al.* Myocardial 123metaiodobenzylguanidine uptake in genetic Parkinson's disease. *Movement Disorders* 2008; **23**: 21–27.
  26. Li ST, Dendi R, Holmes C, Goldstein DS. Progressive loss of cardiac sympathetic innervation in Parkinson's disease. *Annals of Neurology* 2002; **52**: 220–223.

## FULL-LENGTH ORIGINAL RESEARCH

# Negative motor seizure arising from the negative motor area: Is it ictal apraxia?

\*Akio Ikeda, †Ken-ichi Hirasawa, \*Masako Kinoshita, \*Takefumi Hitomi,  
\*Riki Matsumoto, \*Takahiro Mitsueda, ‡§Jun-ya Taki, \*Morito Inouch,  
‡Nobuhiro Mikuni, †Tomokatsu Hori, §Hidenao Fukuyama, ‡Nobuo Hashimoto,  
¶Hiroshi Shibasaki, and \*Ryosuke Takahashi

\*Department of Neurology, Kyoto University School of Medicine, Shogoin, Sakyo-ku, Kyoto, Japan;  
†Department of Neurosurgery, Tokyo Women's Medical University, Tokyo, Japan; ‡Department of Neurosurgery,  
Kyoto University School of Medicine, Shogoin, Sakyo-ku, Kyoto, Japan; §Human Brain Research Center,  
Kyoto University School of Medicine, Shogoin, Sakyo-ku, Kyoto, Japan; and ¶Takeda General Hospital,  
Ishida-mori, Fushimi-ku, Kyoto, Japan

### SUMMARY

**Purpose:** Seizure manifesting motor arrest, that is, negative motor seizure (NMS), is a rare epileptic condition in which only inability to conduct voluntary movements or praxis is produced, although consciousness is preserved. The negative motor area (NMA) seems to be responsible, but its generator mechanism has not yet been clarified.

**Patients and Methods:** Three patients manifesting NMS were investigated. Two patients (ages 33 and 17) with intractable frontal lobe epilepsy had subdural grid implantation for epilepsy surgery, and one (age 77) had scalp electroencephalography (EEG) monitoring.

**Results:** Ictal semiologies commonly observed, at least in the two patients, were found as follows; (1) indescribable or ill-localized aura, (2) repetitive involuntary vocalization, (3) inability to speak, (4) inability to move the extremities, and (5) subse-

quent evolution to positive motor seizures. Awareness and comprehension were preserved throughout the episode before generalized seizures. In two patients with epicortical EEG recording, ictal activity arose from the lateral NMA in one, and from the rostral supplementary motor area in the other. Cortical stimulation at NMA in one patient elicited symptoms identical to NMS. Another patient had scalp EEG and magnetic resonance imaging (MRI) abnormality, both suggesting the epileptogenic focus in the mesial frontal area.

**Conclusion:** We showed that (1) NMS was a rare condition in patients with seizure focus in the frontal lobe, and (2) that the NMA was responsible for the symptoms. The documented state in the present study may reflect ictal apraxia, but it requires further investigation.

**KEY WORDS:** Negative motor seizure, Speech arrest, Negative motor area, Supplementary motor area.

Penfield and Jasper (1954), and later Lüders et al. (1987), reported that a certain cortical area in the frontal cortices produced arrest of voluntary movements, during cortical mapping in patients with intractable partial epilepsy by means of high-frequency electric cortical

stimulation; this cortical area was given the name negative motor area (NMA) (Lüders et al., 1987). It produced the cessation of the voluntary tonic muscle contraction or the rapid alternating movements without loss of awareness, called a negative motor response (NMR).

By contrast, seizure manifesting solely motor arrest without loss of awareness is a rare epileptic condition in which no positive motor symptom but only inability to conduct the voluntary movements is produced, even though consciousness and cognitive function are preserved. It can be called a negative motor seizure (NMS), following NMR because of its similarity. It is entirely

Accepted February 8, 2009; Early View publication May 12, 2009.

Address correspondence to Akio Ikeda, M.D., D.M.S., Department of Neurology, Kyoto University School of Medicine, Shogoin, Sakyo-ku, Kyoto 606, Japan. E-mail: akio@kuhp.kyoto-u.ac.jp. [Correction added after online publication 20 May 2009: Spelling of Morito Inouch changed from Moritoh to Morito below title of paper.]

Wiley Periodicals, Inc.  
© 2009 International League Against Epilepsy

different from focal ictal paresis or ictal monoparesis (Fisher, 1978; Abou-Khalil et al., 1995; So, 1995; Noachtar & Lüders, 1999, 2000; Matsumoto et al., 2005) or epileptic negative myoclonus (Guerrini et al., 1993), which should show mainly weakness or abrupt interruption among continuous muscle contraction, respectively. However, (1) NMS has not been well differentiated from focal ictal paresis, and (2) it has not yet been fully proven whether NMA is responsible for NMS, although semiology of NMS is very similar to NMR produced by cortical stimulation of NMA. In fact, the clinical semiology of seizures from NMA in humans is still uncertain. Previously, three patients with focal "ictal paresis" were reported as having "focal akinetic seizures" (Noachtar & Lüders, 1999). These patients demonstrated an inability to hold the paretic arm outstretched when asked to do so, and they were conscious and speech was not impaired. The two patients had scalp electroencephalography (EEG) monitoring showing the ictal focus in the contralateral central area, and one had subdural EEG recording before epilepsy surgery. EEG disclosed that the ictal onset zone was in the mesial frontal area, possibly corresponding to the supplementary motor area (SMA). Although they could not find the seizure focus in the NMA, they speculated that the ictal onset zone was in the NMA.

Ictal speech arrest due to NMS is also different from ictal aphasia. Aphasic seizure is a well-known, simple partial seizure, which arises from or involves the language areas such as Broca's area (Hamilton & Matthews, 1979), Wernicke's area (Salanova et al., 1995), and basal temporal language area (Kirshner et al., 1995). In addition, ictal speech arrest has been described when the seizures arose from SMA (Penfield & Rasmussen, 1950), but it still remains unresolved whether this condition was produced because of a dysfunction of the NMA within the SMA.

Herein we present three patients who commonly showed ictal motor arrest and/or speech arrest. Two of them had subdural EEG recording, showing ictal activity arising from the NMA in one, and from the rostral SMA in the other. In another patient, scalp EEG and magnetic resonance imaging (MRI) both suggested that the seizure focus was in the mesial frontal area. We showed that (1) NMS is a rare condition in patients with frontal lobe epilepsy or with seizure focus in the frontal lobe, and is different from ictal paresis; (2) the symptoms are often overlooked or unrecognized, and easily masked by the immediately upcoming robust positive motor symptoms; and (3) the NMA is responsible for the symptoms.

Previously the term of NMS was applied to a patient with ictal paresis in a case report (Villani et al., 2006). However, because of the preceding reasons, we will use NMS to describe the rather clear clinical situation based on the present findings, being distinct from ictal paresis.

## PATIENTS AND METHODS

### Patients

We defined NMS as a partial seizure where, by semiology, no positive motor symptoms but only the inability to conduct the voluntary movements or arrest of speech without impairment of comprehension was produced, even though consciousness and cognitive function were preserved. Patients who showed arrest of movements predominantly caused by weakness and decreased tonus of the affected limbs were not included in this study.

Among epileptic patients who had prolonged video-EEG monitoring in the Kyoto University Hospital (KUH) and in the Tokyo Women's Medical University Hospital (TWMUH), three patients presented with NMS. Two of them (Patients 1 and 2) had subdural EEG recording and functional mapping before epilepsy surgery, and another (Patient 3) had scalp EEG recording.

Patient 1 was a 33-year-old, right-handed man with a history of seizures during the 8 months prior to hospitalization. The abstract of the case presentation has been presented previously (Hirasawa et al., 2001). The first seizure occurred as a focal motor seizure involving the tongue, immediately followed by generalized tonic-clonic seizure (GTCS). After treatment with anticonvulsants, the patient had habitual, simple partial seizures occurring every few days as NMS, as described in the Table 1. The patient had no neurologic deficits. The patient had a T<sub>1</sub>-low, T<sub>2</sub>-high-intensity lesion in the left frontal area involving the mesial frontal to the high lateral convexity area (Fig. 1). The subdural electrode grids were implanted before surgery at TWMUH. Finally, the lesion and its surrounding area were resected and the patient had infrequent generalized seizures about three times per year; the pathologic diagnosis was anaplastic astrocytoma.

Patient 2 was a 17-year-old, left-handed man with a history of seizures since the age of 15. The first attack occurred as GTCS. Afterward, GTCSs occurred about once per month with a maximum frequency of seven times per week; these seizures were intractable to medication. The patient initially had a diagnosis of left hand focal motor seizures with Jacksonian march and secondarily GTCSs in the local hospital. He had no focal deficits. The MRI showed a cystic lesion in the right frontal area over the high lateral convexity (Fig. 2). The presence of the lesion, the detailed seizure semiology, and the scalp-recorded ictal EEG finding led us to the diagnosis of intractable right frontal lobe epilepsy. Subdural electrode grids were implanted over the right premotor area at KUH. The epilepsy surgery in this case was described in another paper for an entirely different purpose (Mikuni et al., 2007). The main epileptogenic area was resected and he was free from seizures, except for very brief auras every few months. Pathologic diagnosis was dysembryonic neuroepithelial tumor.

**Table 1. Ictal semiology, MRI findings, and interictal and ictal EEG findings in the three patients**

Patient	1	2	3
Handedness	R	L	R
Age/gender	33/man	17/man	77/woman
Ictal semiology	Indescribable aura <sup>a</sup> Repetitive vocalization <sup>a</sup> Inability to move the limbs <sup>a</sup> and tongue <sup>a</sup>  Speech arrest <sup>b</sup> No loss of awareness <sup>b</sup>	Floating or rising sensation in the whole body <sup>a</sup> Inability to move the whole body <sup>b</sup> Speech arrest <sup>b</sup> No loss of awareness <sup>b</sup> Asymmetric tonic convulsion	Rhythmic vocalization <sup>a</sup> Speech arrest <sup>b</sup> Slow tongue wiggling <sup>a</sup> No loss of awareness <sup>b</sup> Slow movements of the right hand Very mild weakness of the right proximal upper limb
MRI	History of GTCS <sup>a</sup> A T1-low, T2-high, left mesial frontal lesion	History of GTCS <sup>a</sup> A cystic lesion in the right, high lateral premotor area	T <sub>2</sub> -positive abnormality in the left mesial frontal surface
Type of EEG recording/interictal findings	Subdural Frequent spikes at ictal onset zone	Subdural Frequent spikes at ictal onset zone	Scalp Frequent spikes at Cz
Type of EEG recording/ictal findings	Subdural A2 showed 100-Hz burst activity, and then A2 and adjacent three electrodes showed 7–8 Hz spikes	Subdural Three electrodes initially showed 8–12 Hz rhythmic activities	Scalp No definite changes
Focus location: in relation to NMA	No NMA defined seizures arose from SMA close to VAC	Five electrodes defined as NMA, from which seizures arose	Most likely located on the SMA

GTCS, generalized tonic-clonic seizures, MRI, magnetic resonance imaging; L, left; EEG, electroencephalography; NMA, negative motor area; R, right; SMA, supplementary motor area; VAC, a line on the anterior commissure vertical to AC-PC line (a line crossing anterior commissure and posterior commissure line).

<sup>a</sup>Observed in two patients. <sup>b</sup>Observed in three patients.

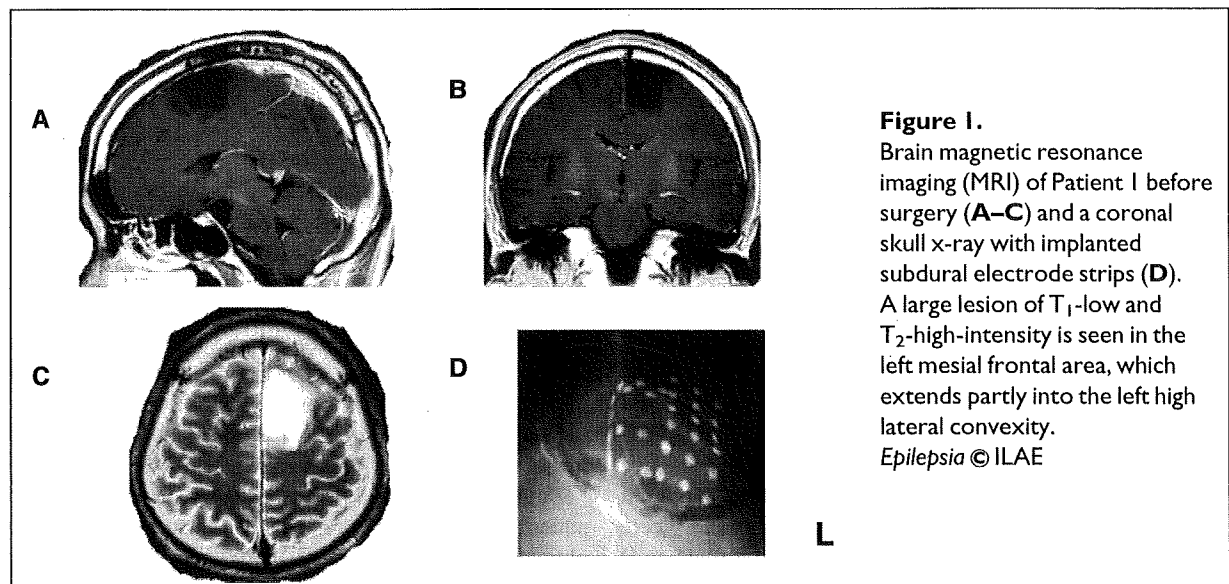


**Figure 1.** Brain magnetic resonance imaging (MRI) of Patient 1 before surgery (A–C) and a coronal skull x-ray with implanted subdural electrode strips (D). A large lesion of T<sub>1</sub>-low and T<sub>2</sub>-high-intensity is seen in the left mesial frontal area, which extends partly into the left high lateral convexity. *Epilepsia* © ILAE

Patient 3 was a 77-year-old, right-handed woman who was admitted to KUH because of frequent attacks of inability to speak. Twenty days before admission the patient hit the occipital region of her head on the floor at home. She did not lose her consciousness but after half an hour her speech was incoherent. Three days later, the patient started having episodes of being unable to speak. The episodes lasted from several seconds to a minute. The

episodes increased in frequency and occurred 30 times per day. On admission, the patient was alert interictally and well-oriented. No motor or sensory impairments were observed. The patient had had no previous convulsions. Cranial computed tomography (CT) scan revealed a mild subdural effusion with slightly increased CT density throughout the left hemisphere (Fig. 3A). Cranial MRI showed a similar finding (Fig. 3B), and T<sub>2</sub>- and